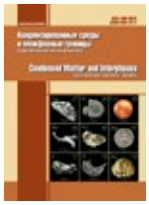

ISSN 1606-867X (Print)
ISSN 2687-0711 (Online)
Condensed Matter and Interphases
Kondensirovannye Sredy i Mezhfaznye Granitsy
https://journals.vsu.ru/kcmf/

**Original articles**

Research article
https://doi.org/10.17308/kcmf.2024.26/11946

# Synthesis and sensory properties of tungsten (VI) oxide-based nanomaterials

**A. V. Shaposhnik[1]✉, A. A. Zvyagin[1], S. V. Ryabtsev[2], O. V. Dyakonova[1], E. A. Vysotskaya[1]**

*[1]Voronezh State Agrarian University*
*1 Michurin str., Voronezh 394087 Russian Federation*

*[2] Voronezh State University,*
*1 Universitetskaya pl., Voronezh 394018, Russian Federation*

**Abstract**

The purpose of this work was to develop a methodology for the synthesis of $WO_3$-based nano-scale materials, to provide their characterization, and to study their sensory properties.

The nanopowder was made by slowly adding nitric acid to an aqueous solution of ammonium paratungstate, $(NH_4)_{10}W_{21}O_{41}{\cdot}xH_2O$, followed by centrifugation, drying, and calcination. The size of tungsten trioxide grains, which was 10-20 nm, was determined by transmission electron microscopy. According to X-ray phase analysis, the powder, which was calcined at a temperature of 500 °C, mainly consisted of a triclinic phase. Subsequently, diammine palladium (II) nitrate and terpeniol were added to the $WO_3$ nanopowder to form a paste. The resulting paste was applied to a special dielectric substrate and calcined to a temperature of 750 °C. As a result, a fragile tungsten trioxide-based gel formed. The mass fraction of palladium in the fragile gel was 3%. The sensory properties of the obtained gas-sensitive material were studied under stationary (300 °C) and non-stationary temperature conditions (quick heating to 450 °C and slow cooling to 100 °C).

A sharp increase in the sensitivity of a tungsten trioxide-based sensor was observed under non-stationary temperature conditions which depended on the composition of the gas-sensitive layer.

**Keywords:** MOX sensor; Sensitivity; Temperature modulation

***Acknowledgements:*** The study was supported by the Russian Science Foundation grant (project No. 23-23-00329).

***For citation:*** Shaposhnik A. V, Zviagin A. A., Ryabtsev S. V., Dyakonova O. V., Vysotskaya E. A. Synthesis and sensory properties of tungsten (VI) oxide-based nanomaterials. *Condensed Matter and Interphases*. 2023;24(2): 349–355. https://doi.org/10.17308/kcmf.2024.26/11946

***Для цитирования:*** Шапошник А. В., Звягин А. А., Рябцев С. В., Дьяконова О. В., Высоцкая Е. А. Синтез и сенсорные свойства наноматериалов на основе оксида вольфрама (VI). *Конденсированные среды и межфазные границы*. 2023;24(2): 349–355. https://doi.org/10.17308/kcmf.2024.26/11946

✉ Alexey V. Shaposhnik, e-mail: a.v.shaposhnik@gmail.com


## 1. Introduction

Tungsten trioxide is a semiconductor with a band gap of 2.4–2.8 eV [1]. The application of $WO_3$ is quite wide: for example, it is used to manufacture scintillators, luminophores, and electrochromic glass that can change light transmission with the changes in electrical voltage. Tungsten trioxide-based materials are used as hydrogenation catalysts during hydrocarbon cracking. Recently, nanodispersed tungsten (VI) oxide has become widely used as a gas-sensitive material for chemical sensors [2].

In most cases, $WO_3$ is the basis of the gas-sensitive material, while additives increase sensitivity and selectivity. For example, a highly sensitive acetone sensor was obtained from the $WO_3$/Au nanocomposite [3]. The mesoporous sensor based on the $WO_3$-$TiO_2$ heterojunction is highly sensitive to hydrogen [4]. A sensor with a p-n heterojunction at the boundary of NiO nanosheets and $WO_3$ nanorods has a high sensitivity to acetaldehyde [5].

Sensors with very low power consumption can be created using individual metal oxide nanofilaments [6]. A very fast nanosecond response and extremely low power consumption at the level of several microwatts was achieved using an individual $WO_3$ nanofilament coated with platinum [7]. The mechanism of chemical processes involved in detection of hydrogen in air was investigated using a gas-sensitive material consisting of $WO_3$ nanorods [8]. The *p*-$NiCo_2O_4$/*n*-$WO_3$ heterojunction was used to obtain a sensor with high sensitivity to nitrogen dioxide [9]. In addition, a NOx sensor was created based on palladium doped $WO_3$ [10]. Doping of a n-type semiconductor, $WO_3$ nanospheres, with a p-type semiconductor (antimony) made it possible to obtain an ammonia sensor operating at a temperature close to room temperature [11].

Flower-like $WO_3$-$In_2O_3$ hollow microspheres were used as a gas-sensitive material used to detect acetone [12]. Iron doped reduced graphene oxide (rGO) was added to $WO_3$ to create a low temperature acetone sensor [13]. A sensor capable of detecting amines at the level of ppb concentrations was created using $WO_3$-$W_{18}O_{49}$ heterostructures with the addition of graphene layers and PdO nanoparticles [14].

A $WO_3$/$CuWO_4$ heterostructure with 3D hierarchical pores was used to create a highly sensitive sensor operating at room temperature under the influence of visible radiation [15]. A Pd-$WO_3$ sensor with reinforced "self-assembly" made it possible to detect hydrogen even at room temperature [16].

A chemoresistive $NO_2$ sensor using lanthanum doped $WO_3$ was synthesized by flame spray pyrolysis [17]. A highly sensitive and highly selective $H_2S$ sensor based on a flower-like $WO_3$/CuO nanocomposite can operate at low temperatures close to room temperature [18].

An ultra-low detection limit for ammonia detection at room temperature was achieved for a nanocomposite consisting of $WO_3$ and multi-walled carbon nanotubes (MWCNT) [20]. A low-temperature $WO_3$-$Bi_2WO_6$ sensor with a hierarchical flower-like structure made it possible to detect $H_2S$ at the level of ppb concentrations [21]. A fast responding and highly reversible hydrogen sensor was obtained by doping amorphous $WO_3$ thin films with palladium [22]. $WO_3$-decorated $TiO_2$-based nanofiber allowed obtaining a heterostructure with high sensitivity to hydrogen [23]. Surface modification of the $WO_3$ nanomaterial with Pt and Ru particles was used to obtain sensors sensitive to vapors of low-boiling liquids [24]. A $WO_3$-PdO core-shell architecture was used to obtain a highly sensitive acetone sensor [25].

The sensory properties of $WO_3$-based nanofilms obtained by magnetron sputtering have been studied in detail [26]. $WO_3$ nanofilms can also be prepared by thermal oxidation of metallic tungsten, however, its responses to nitrogen oxides and ammonia were not very high [27]. A micro-machined $WO_3$-based sensor was created to detect oxidizing gases. Importantly, the authors managed to achieve not only high responses, but also high selectivity by processing the results by the "electronic nose" methodology [28]. A highly sensitive hydrogen sensor was created by co-spraying tungsten and platinum [29].

One of the greatest challenges related to gas analysis with the help of sensors is their insufficient selectivity [30], which can be increased using a non-stationary temperature conditions of the sensor [31–33].

The purpose of this work was to synthesize $Wo_3$-based nanomaterials, to provide their characterization, and to study their sensory properties in relation to hydrogen sulfide and carbon monoxide. In addition, the purpose of this study was to compare two temperature conditions: stationary and non-stationary.

## 2. Experimental

### *2.1. Synthesis and characterization of the gas-sensitive material*

6.25 g of ammonium paratungstate (Sigma-Aldrich, Product Number 510114, Batch number MKCL8549) was dissolved in 250 ml of deionized water at 80 °C. Further, 3M nitric acid solution was added dropwise to the constantly stirred solution until pH = 0. The temperature was maintained at 80 °C. The resulting mixture was kept at 80 °C for 30 minutes and then cooled to room temperature and kept for one hour.

$$(NH_4)_{10}W_{12}O_{41}\cdot 5H_2O + 10HNO_3 + 2H_2O \rightarrow \rightarrow 12H_2WO_4\downarrow + 10NH_4NO_3. \quad (1)$$

The tungstic acid precipitate was separated by centrifugation, washed with deionized water, and dried at 80 °C for 12 hours. As a result of further heat treatment of the dried tungstic acid precipitate for 24 hours at a temperature of 500 °C, tungsten trioxide formed:

$$H_2WO_4 \rightarrow WO_3 + H_2O. \quad (2)$$

The tungsten trioxide nanopowder was characterized by transmission electron microscopy (Fig. 1) and by X-ray phase analysis (XRD) using a DRON-4 device with a cobalt anode (Fig. 2). According to the electron microscopy data, the size of $WO_3$ grains was 10–20 nm. The diffraction pattern was interpreted using the Powder Diffraction File (PDF-2) database. The PDF data for hexagonal and triclinic modifications of $WO_3$ were plotted to the left side of Y-axis. The experimental XRD data were plotted to the right side of Y-axis. It was found that the sample

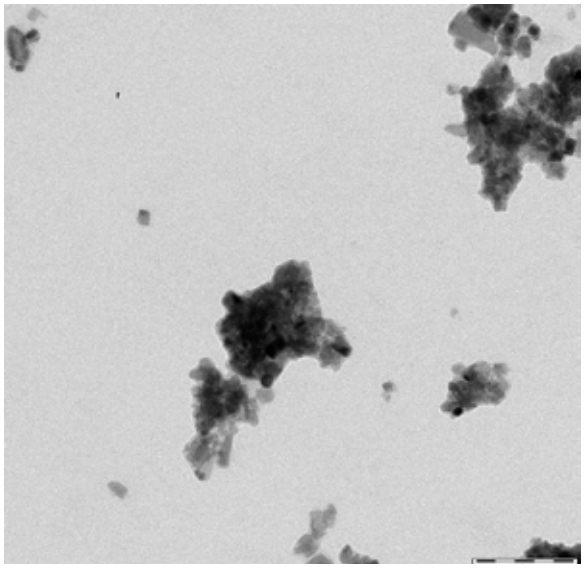

**Fig. 1.** Transmission electron microscopy image of tungsten (VI) oxide nanopowder

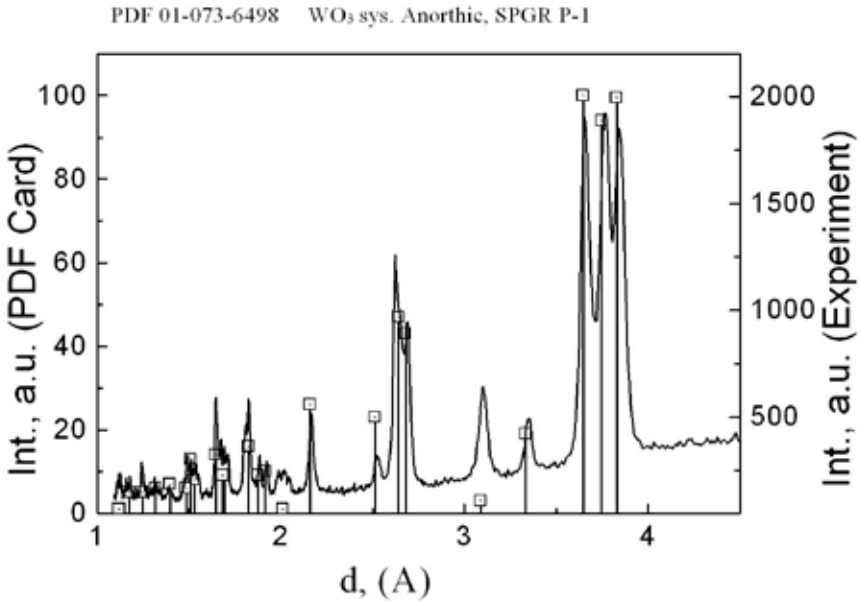


**Fig. 2.** X-ray diffraction pattern of tungsten (VI) oxide nanopowder calcinated at 500 °C

corresponded to the triclinic phase of $WO_3$ (PDF card 01-073-6498).

A gas-sensitive layer based on $WO_3$ with the addition of palladium oxide was obtained by treating tungsten trioxide powder with a solution of tetraammine palladium (II) nitrate with the addition of terpeniol as a binder component. The resulting paste was applied on a dielectric substrate made of aluminum oxide with platinum electrodes and a heater, then it was calcined to a temperature of 750 °C. As a result, terpeniol burned out and a layer of tungsten trioxide with the addition of palladium oxide in the form of a gel formed on the substrate.

### *2.2. Measuring sensory characteristics*

Control gas mixtures "hydrogen sulfide in synthetic air" and "carbon monoxide in synthetic air" with concentrations of 10 ppm and 200 ppm diluted with synthetic air at a flow rate of 250 ml/min were used to study the sensory properties of the obtained materials. A metal-enclosed TO-8 sensor was placed in a stainless steel chamber. The temperature of the sensor was set by a special electronic device according to the temperature coefficient of resistance of the heater.

The electrical resistivity of the gas-sensitive layer of the sensor was measured with a special electronic device with a sampling rate of 40 Hz and recorded as a computer file. Each measurement cycle lasted 15 seconds: 2 seconds of heating from 100 to 450 °C and then 13 seconds of cooling from 450 to 100 °C. These cycles were continuous (Fig. 3). The results of the first five cycles of measurements were not taken into account. Only one of the 575 cycle points was used for quantitative determination, which corresponded to a time of 14.95 seconds after the start of the measurements.

The response S was calculated by the ratio of the active electrical resistance $R_0$ in clean air to the active electrical resistance $R_g$ in the studied gas medium according to the formula:

$$S = R_0/R_g. \quad (3)$$

## 3. Results and discussion

The sensor temperature (curve *1*) and the electrical resistivity of the $WO_3$-Pd sensor when detecting carbon monoxide (curve *2*) and hydrogen sulfide (curve *3*) over three measurement cycles are shown in Fig. 3.

Fig. 4 shows the concentration dependences of the electrical resistance of the $WO_3$-Pd sensor on time during one measurement cycle for hydrogen sulfide.

Fig. 5 shows the dependence of the $WO_3$-Pd sensor response on the concentration of hydrogen sulfide in stationary (curve *1*) and non-stationary temperature conditions (curve *2*). According to the figure, the non-stationary conditions

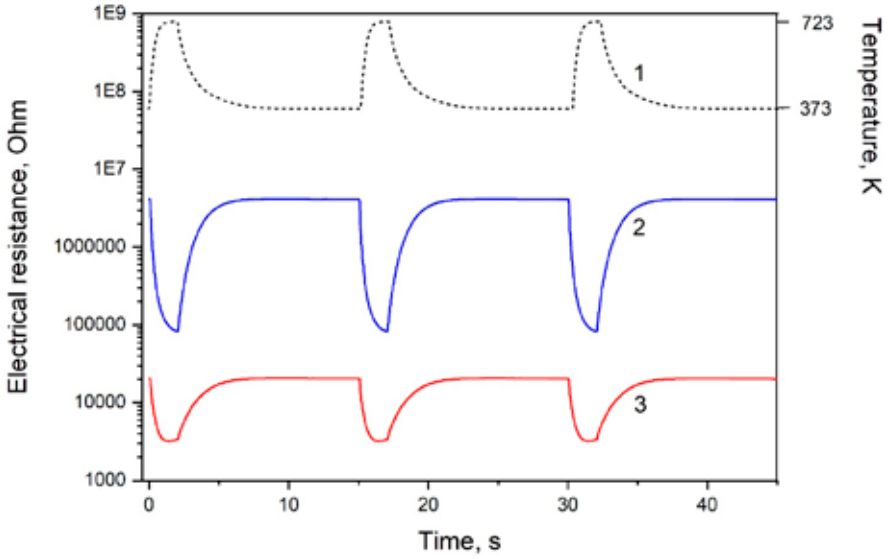


**Fig. 3.** Temperature (curve *1*) and the electrical resistance of the $WO_3$-Pd sensor at 50 ppm carbon monoxide (curve *2*) and at 50 ppm hydrogen sulfide (curve *3*) in a non-stationary temperature regime over three measurement cycles

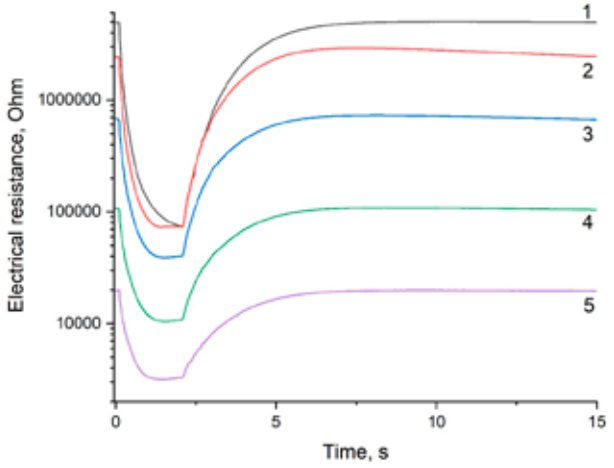


**Fig. 4.** Electrical resistance of $WO_3$-Pd sensor in hydrogen sulfide of various concentrations at a non-stationary temperature condition during one measurement cycle. *1* – synthetic air, *2* – 5 ppm $H_2S$, *3* – 10 ppm $H_2S$, *4* – 20 ppm $H_2S$, *5* – 50 ppm $H_2S$

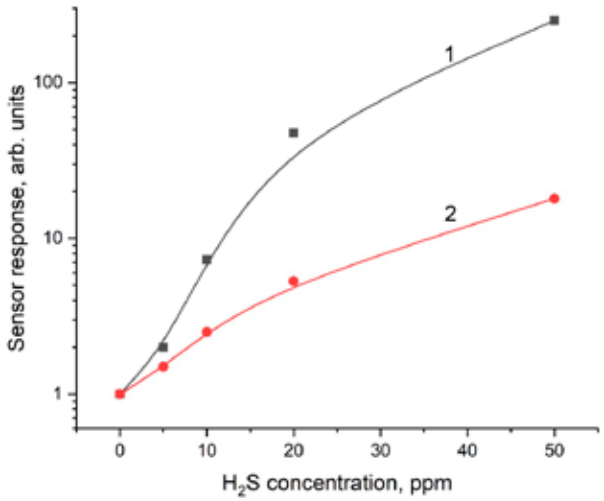


**Fig. 5.** Dependence of the response of the $WO_3$-Pd sensor on the concentration of hydrogen sulfide in non-stationary mode (*1*) and at a stationary temperature of 300 °C (*2*)

contribute to an increase in the sensor response to hydrogen sulfide by about an order of magnitude. The difference in the form of sensor resistance versus time dependences when detecting carbon monoxide and hydrogen sulfide can be used to increase the analysis selectivity [33].

An increase in the sensitivity of the $WO_3$-Pd sensor to hydrogen sulfide may be explained by the temporary separation of the catalytic activity of the gas-sensitive layer of the sensor and the sorption of the analyte gas [31]. The non-stationary temperature conditions seem to activate the gas-sensitive layer of the sensor before the analyte gas desorption begins. In addition, the sensor response also depends on the total concentration of the charge carriers. The higher the sensor response, the fewer charge carriers are present in the metal oxide sensor before the analyte gas is released. As a result, the impulsed temperature changes increase the resistance of the $WO_3$-Pd sensor in air due to high oxygen sorption.

## 4. Conclusions

As a result of the study, the traditional sol-gel technology was used to produce a $WO_3$-Pd sensor by adding palladium oxide (3% by weight) to a tungsten trioxide nanopowder. The sensory characteristics of the resulting material in relation to hydrogen sulfide and carbon monoxide were investigated. The conducted studies of sensory characteristics in two types of temperature conditions showed that the impulsed temperature changes result in a significant increase in the sensitivity of the sensor to hydrogen sulfide. Therefore, when operating in non-stationary temperature conditions, the $WO_3$-Pd sensor can be used to detect hydrogen sulfide and other reducing gases.

## Contribution of the authors

The authors contributed equally to this article.

## Conflict of interests

The authors declare that they have no known competing financial interests or personal relationships that could have influenced the work reported in this paper.

## References

1. Tesfamichael T., Ponzoni A., Ahsan M., Faglia G. Gas sensing characteristics of Fe-doped tungsten oxide thin films. *Sensors and Actuators B: Chemical*. 2012;168(2): 345–353. https://doi.org/10.1016/j.snb.2012.04.032

2. Tesfamichael T., Ahsan M., Notarianni M., … Bell J. Gas sensing of ruthenium implanted tungsten oxide thin films. *Thin Solid Films*. 2014;558: 416–422. https://doi.org/10.1016/j.tsf.2014.02.084

3. Zhang X., Dong B., Liu W., … Song H. Highly sensitive and selective acetone sensor based on three-dimensional ordered $WO_3$/Au nanocomposite with

enhanced performance. *Sensors Actuators, B Chemical*. 2020;320(4): 128405. https://doi.org/10.1016/j.snb.2020.128405

4. Li H., Wu C.-H., Liu Y.-C., … Wu R.-J. Mesoporous $WO_3$-$TiO_2$ heterojunction for a hydrogen gas sensor. *Sensors Actuators, B Chemical*. 2021;341(2): 130035. https://doi.org/10.1016/j.snb.2021.130035

5. Nakate U. T., Yu Y. T., Park S. High performance acetaldehyde gas sensor based on *p-n* heterojunction interface of NiO nanosheets and $WO_3$ nanorods. *Sensors Actuators, B Chemical*. 2021;344(5): 130264. https://doi.org/10.1016/j.snb.2021.130264

6. Shaposhnik A. V., Shaposhnik D. A., Turishchev S. Y., … Morante J. R. Gas sensing properties of individual $SnO_2$ nanowires and $SnO_2$ sol-gel nanocomposites. *Beilstein Journal of Nanotechnology*. 2019;10: 1380–1390. https://doi.org/10.3762/bjnano.10.136

7. Fan L., Xu N., Chen H., Zhou J., Deng S. A millisecond response and microwatt power-consumption gas sensor: Realization based on cross-stacked individual Pt-coated $WO_3$ nanorods. *Sensors Actuators B Chemical*. 2021;346(2): 130545. https://doi.org/10.1016/j.snb.2021.130545

8. Mineo G., Moulaee K., Neri G., Mirabella S., Bruno E. $H_2$ detection mechanism in chemoresistive sensor based on low-cost synthesized $WO_3$ nanorods. *Sensors Actuators B Chemical*. 2021;348: 130704. https://doi.org/10.1016/j.snb.2021.130704

9. Hu Y., Li T., Zhang J., Guo J., Wang W., Zhang D. High-sensitive $NO_2$ sensor based on *p*-$NiCo_2O_4$/*n*-$WO_3$ heterojunctions. *Sensors Actuators B Chemical*. 2022;352(P2): 130912. https://doi.org/10.1016/j.snb.2021.130912

10. Karpe S. B., Bang A. D., Adhyapak D. P., Adhyapak P. V. Fabrication of high sensitive proto-type NOx sensor based on Pd nanoparticles loaded on $WO_3$. *Sensors Actuators B Chemical*. 2022;354: 131203. https://doi.org/10.1016/j.snb.2021.131203

11. Yao G., Yu J., Wu H., … Tang Z. *P*-type Sb doping hierarchical $WO_3$ microspheres for superior close to room temperature ammonia sensor. *Sensors Actuators B Chemical*. 2022;359: 131365. https://doi.org/10.1016/j.snb.2022.131365

12. Hu J., Xiong X., Guan W., Long H., Zhang L., Wang H. Self-templated flower-like $WO_3$-$In_2O_3$ hollow microspheres for conductometric acetone sensors. *Sensors Actuators B Chemical*. 2022;361(10): 131705. https://doi.org/10.1016/j.snb.2022.131705

13. Sen S., Maity S., Kundu S. Fabrication of Fe doped reduced graphene oxide (rGO) decorated $WO_3$ based low temperature ppm level acetone sensor: Unveiling sensing mechanism by impedance spectroscopy. *Sensors Actuators B Chemical*. 2022;361(3): 131706. https://doi.org/10.1016/j.snb.2022.131706

14. Wang X., Han W., Yang J., … Lu G. Conductometric ppb-level triethylamine sensor based on macroporous $WO_3$-$W_{18}O_{49}$ heterostructures functionalized with carbon layers and PdO nanoparticles. *Sensors Actuators B Chem*. 2022;361(1): 131707. https://doi.org/10.1016/j.snb.2022.131707

15. Liu Y., Li X., Li X., … Liu Y. Highly permeable $WO_3$/$CuWO_4$ heterostructure with 3D hierarchical porous structure for high-sensitive room-temperature visible-light driven gas sensor. *Sensors Actuators B Chemical*. 2022;365(4): 131926. https://doi.org/10.1016/j.snb.2022.131926

16. Lee J., Kim S. Y., Yoo H. S., Lee W. Pd-$WO_3$ chemiresistive sensor with reinforced self-assembly for hydrogen detection at room temperature. *Sensors Actuators B Chemical*. 2022;368(6): 132236. https://doi.org/10.1016/j.snb.2022.132236

17. Zhang Y., Wu C., Xiao B., … Lin H. Chemo-resistive $NO_2$ sensor using La-doped $WO_3$ nanoparticles synthesized by flame spray pyrolysis. *Sensors Actuators B Chemical*. 2022;369:(2): 132247. https://doi.org/10.1016/j.snb.2022.132247

18. He M., Xie L., Zhao X., Hu X., Li S., Zhu Z.-G. Highly sensitive and selective $H_2S$ gas sensors based on flower-like $WO_3$/CuO composites operating at low/room temperature. *Journal of Alloys and Compounds*. 2019;788: 36–43. https://doi.org/10.1016/j.jallcom.2019.01.349

19. Marikutsa A., Yang L., Kuznetsov A. N., Rumyantseva M., Gaskov A. Effect of W–O bonding on gas sensitivity of nanocrystalline $Bi_2WO_6$ and $WO_3$. *Journal of Alloys and Compounds*. 2021;856: 158159. https://doi.org/10.1016/j.jallcom.2020.158159

20. Duong V. T., Nguyen C. T., Luong H. B., Nguyen D. C., Nguyen H. L. Ultralow-detection limit ammonia gas sensors at room temperature based on MWCNT/$WO_3$ nanocomposite and effect of humidity. *Solid State Sciences*. 2021;113(11): 106534. https://doi.org/10.1016/j.solidstatesciences.2021.106534

21. Zhang C., Wu K., Liao H., Debliquy M. Room temperature $WO_3$-$Bi_2WO_6$ sensors based on hierarchical microflowers for ppb-level $H_2S$ detection. *Chemical Engineering Journal*. 2022;430(P2): 132813. https://doi.org/10.1016/j.cej.2021.132813

22. Hwan Cho S., Min Suh J., Jeong B., … Won Jang H. Fast responding and highly reversible gasochromic $H_2$ sensor using Pd-decorated amorphous $WO_3$ thin films. *Chemical Engineering Journal*. 2022;446(P1): 136862. https://doi.org/10.1016/j.cej.2022.136862

23. Kumaresan M., Venkatachalam M., Saroja M., Gowthaman P. $TiO_2$ nanofibers decorated with monodispersed $WO_3$ heterostruture sensors for high gas sensing performance towards $H_2$ gas. *Inorganic Chemistry Communications*. 2021;129(2): 108663. https://doi.org/10.1016/j.inoche.2021.108663

24. Chen L., Zhang Y., Sun B., … Tian C. Surface modification of $WO_3$ nanoparticles with Pt and Ru for VOCs sensors. *Chinese Journal of Analytical Chemistry*. 2022: 100143. https://doi.org/10.1016/j.cjac.2022.100143

25. Hu J., Xiong X., Guan W., Long H. Designed construction of PdO@$WO_3$ core–shell architecture as a high-performance acetone sensor. *Journal of Environmental Chemical Engineering*. 2021;9(6): 106852. https://doi.org/10.1016/j.jece.2021.106852

26. *Sensor electronics, sensors: solid state sensors on silicon: a study guide for students of higher education institutions* / E. P. Domashevskaya [et al.]; edited by A. M. Hoviv. Moscow: Yurayt Publishing House, 2020. 203 p. (in Russ). Available at: https://urait.ru/bcode/518779

27. Siciliano T., Tepore A., Micocci G., Serra A., Manno D., Filippo E. $WO_3$ gas sensors prepared by thermal oxidization of tungsten. *Sensors and Actuators B: Chemical*. 2008;133(1): 321–326. https://doi.org/10.1016/j.snb.2008.02.028

28. Vallejos S., Khatko V., Calderer J., … Correig X. Micro-machined $WO_3$-based sensors selective to oxidizing gases. *Sensors and Actuators B: Chemical*. 2008;132(1): 209–215. https://doi.org/10.1016/j.snb.2008.01.044

29. Zhang C., Boudiba A., Navio C., … Debliquy M. Highly sensitive hydrogen sensors based on co-sputtered platinum-activated tungsten oxide films. *International Journal of Hydrogen Energy*. 2010;36(1): 1107–1114. https://doi.org/10.1016/j.ijhydene.2010.10.011

30. Yakovlev P. V., Shaposhnik A. V., Voishchev V. S., Kotov V. V., Ryabtsev S. V. Determination of gases using polymer-coated semiconductor sensors. *Journal of Analytical Chemistry*. 2002;57(3): 276–279. https://doi.org/10.1023/A:1014412919822

31. Shaposhnik A. V., Moskalev P. V., Zviagin A. A., … Vasiliev A. A. Selective determination of hydrogen sulfide using $SnO_2$–Ag sensor working in non-stationary temperature regime. *Chemosensors*. 2021;9(8): 203. https://doi.org/10.3390/chemosensors9080203

32. Shaposhnik A., Zvyagin A., Vasiliev A., Ryabtsev S., Shaposhnik D., Nazarenko I., Buslov V. Optimal temperature regimes of semiconductor sensors determination. *Sorbtsionnye i Khromatograficheskie Protsessy*. 2008;8(3): 501–506. (In Russ., abstract in Eng.). Available at: https://www.elibrary.ru/item.asp?id=11928774

33. Shaposhnik A., Moskalev P., Sizask E., Ryabtsev S., Vasiliev A. Selective detection of hydrogen sulfide and methane by a single MOX-sensor. *Sensors (Switzerland)*. 2019;19(5): 1135. https://doi.org/10.3390/s19051135

## Information about the authors

*Alexey V. Shaposhnik,* Dr. Sci. (Chem.), Professor at the Department of Chemistry, Voronezh State Agrarian University (Voronezh, Russian Federation).

https://orcid.org/0000-0002-1214-2730

a.v.shaposhnik@gmail.com

*Alexey A. Zviagin,* Cand. Sci. (Chem.), Associate Professor at the Department of Chemistry, Voronezh State Agrarian University (Voronezh, Russian Federation).

https://orcid.org/0000-0002-9299-6639

a.a.zviagin@rambler.ru

*Stanislav V. Ryabtsev,* Dr. Sci. (Phys.–Math.), Head of the Laboratory, Voronezh State University, (Voronezh Russian Federation).

https://orcid.org/0000-0001-7635-8162

raybtsev@niif.vsu.ru

*Olga V. Dyakonova,* Cand. Sci. (Chem.), Associate Professor at the Department of Chemistry, Voronezh State Agrarian University (Voronezh, Russian Federation).

dyakol@yandex.ru

*Elena A. Vysotskaya*, Dr. Sci. (Biol.), Dean of the Faculty of Technology and Commodity Science, Voronezh State Agrarian University (Voronezh, Russian Federation).

murka1979@mail.ru

*Received 03.06.2023; approved after reviewing 03.09.2023; accepted for publication 15.09.2023; published online 25.06.2024.*

*Translated by Irina Charychanskaya*